Corrections

BIOCHEMISTRY

Correction for "Enhancing nuclear receptor-induced transcription requires nuclear motor and LSD1-dependent gene networking in interchromatin granules," by Qidong Hu, Young-Soo Kwon, Esperanza Nunez, Maria Dafne Cardamone, Kasey R. Hutt, Kenneth A. Ohgi, Ivan Garcia-Bassets, David W. Rose, Christopher K. Glass, Michael G. Rosenfeld, and Xiang-Dong Fu, which appeared in issue 49, December 9, 2008, of *Proc Natl Acad Sci USA* (105:19199–19204; first published December 3, 2008; 10.1073/pnas.0810634105).

The authors wish to note, "The legend of Fig. 2*B* should state that the experiment was performed in HMEC cells, rather than in MCF7 cells, similar to the confirmatory experiment presented in Fig. 2*C*." The figure and its corrected legend appear below.

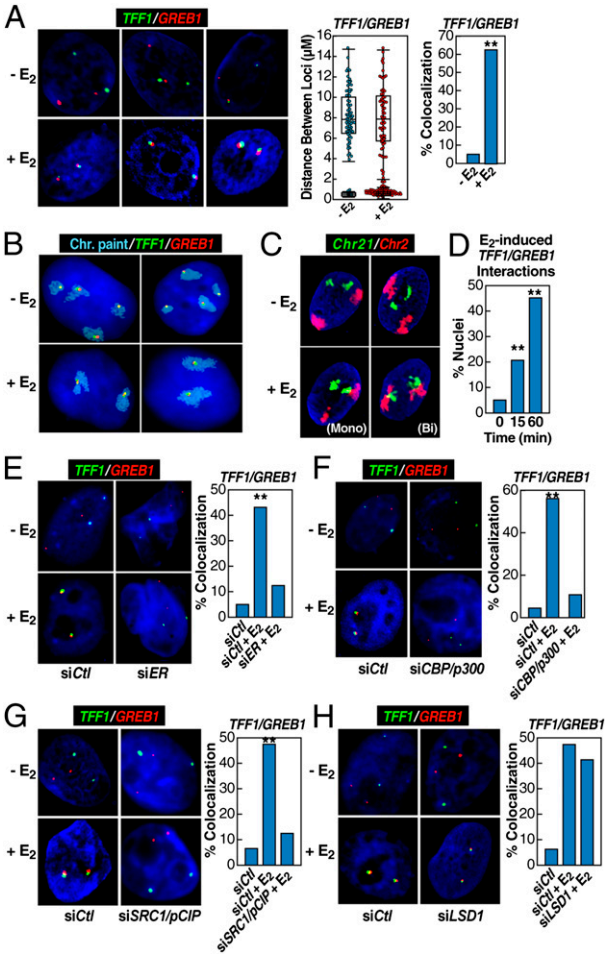

Fig. 2. Rapid induction of interchromosomal interactions by nuclear hormone signaling. (*A*) 3D-FISH confirmation of E_2-induced (60 min) *TFF1:GREB1* interchromosomal interactions in HMECs with the distribution of loci distances measured (box plot with scatter plot) and quantification of colocalization (bar graph) before and after E_2 treatment. Cells exhibiting mono- or biallelic interactions were combined for comparison with cells showing no colocalization; statistical significance in the bar graph was determined by χ^2 test (**, $P < 0.001$). (*B*) 2D FISH confirmation of the interchromosomal interactions in HMEC cells by combining chromosome paint (aqua) and specific DNA probes (green and red). (*Upper*) Illustrates two examples of mock-treated cells. (*Lower*) Shows the biallelic interactions/nuclear reorganization after E_2 treatment for 60 min, exhibiting kissing events between chromosome 21 and chromosome 2. (*C*) Similar analysis on HMECs, but in this case using 3D FISH to paint chromosome 2 (red) and chromosome 21 (green), showing E_2-induced chromosome 2–chromosome 21 interaction. Both assays revealed neither chromosome 21–chromosome 21 nor chromosome 2–chromosome 2 interactions in response to E_2. (*D*) Temporal kinetics of *GREB1*:*TFF1* interactions by 3D FISH in HMECs (**, $P < 0.001$ by χ^2). (*E–G*) Nuclear microinjection of siRNA against *ERα*, *CBP/p300*, or *SRC1/pCIP* prevented E_2-induced interchromosomal interactions, counting both mono- and biallelic interactions (**, $P < 0.001$ by χ^2). The injection of *siER* and *siDLC1* were done in the same experiment, sharing the same control group. (*H*) Nuclear microinjection of siRNA against *LSD1*, which was shown to be required for estrogen-induced gene expression (22), did not block E_2-induced interchromosomal interactions. The injection of *siLSD1* and *SRC1/pCIP* were done in a single experiment, sharing the same control group.

www.pnas.org/cgi/doi/10.1073/pnas.1400054111

BIOCHEMISTRY

Update to Correction for "Confinement of caspase-12 proteolytic activity to autoprocessing," by Sophie Roy, Jeffrey R. Sharom, Caroline Houde, Thomas P. Loisel, John P. Vaillancourt, Wei Shao, Maya Saleh, and Donald W. Nicholson, which appeared in issue 11, March 18, 2008, of *Proc Natl Acad Sci USA* (105:4133–4138; first published March 10, 2008; 10.1073/pnas.0706658105).

The authors wish to note: "We recently published corrections to two articles that describe the functional role (1) and enzymology (2) of caspase-12. The figures in these two articles have been thoroughly investigated by a committee at McGill University. With regard to Fig. 6 in the article in PNAS, two findings were determined: First, that republication of the data was a consequence of miscommunication among co-authors working in different locations, and second, that the molecular weight markers were unintentionally mislabeled. The latter issue has recently been corrected (3). The former issue has recently been rectified because figure 4 of the *Nature* article was replaced with a *de novo* independent experiment (4). Interpretation of the experiment and the conclusions of both the PNAS article and the *Nature* article are unaffected by these changes. The authors apologize for any confusion."

1. Saleh M, et al. (2006) Enhanced bacterial clearance and sepsis resistance in caspase-12-deficient mice. *Nature* 440(7087):1064–1068.
2. Roy S, et al. (2008) Confinement of caspase-12 proteolytic activity to autoprocessing. *Proc Natl Acad Sci USA* 105(11):4133–4138.
3. Roy S, et al. (2013) Correction: Confinement of caspase-12 proteolytic activity to autoprocessing. *Proc Natl Acad Sci USA* 110(12):4852.
4. Saleh M, et al. (2013) Corrigendum: Enhanced bacterial clearance and sepsis resistance in caspase-12-deficient mice. *Nature*, 10.1038/nature12181.

www.pnas.org/cgi/doi/10.1073/pnas.1323789111

IMMUNOLOGY

Correction for "MicroRNA-directed program of cytotoxic CD8+ T-cell differentiation," by Sara Trifari, Matthew E. Pipkin, Hozefa S. Bandukwala, Tarmo Äijö, Jed Bassein, Runqiang Chen, Gustavo J. Martinez, and Anjana Rao, which appeared in issue 46, November 12, 2013, of *Proc Natl Acad Sci USA* (110:18608–18613; first published October 25, 2013; 10.1073/pnas.1317191110).

The authors note that the accession number for the GEO database is GSE51393.

www.pnas.org/cgi/doi/10.1073/pnas.1400120111

MEDICAL SCIENCES, ENGINEERING

Correction for "Generation of functionally competent and durable engineered blood vessels from human induced pluripotent stem cells," by Rekha Samuel, Laurence Daheron, Shan Liao, Trupti Vardam, Walid S. Kamoun, Ana Batista, Christa Buecker, Richard Schäfer, Xiaoxing Han, Patrick Au, David T. Scadden, Dan G. Duda, Dai Fukumura, and Rakesh K. Jain, which appeared in issue 31, July 30, 2013, of *Proc Natl Acad Sci USA* (110:12774–12779; first published July 16, 2013; 10.1073/pnas.1310675110).

The authors note that the following statement should be added to the Acknowledgments: "This work is in part supported by Department of Defense (DoD) Breast Cancer Research Innovator Award W81XWH-10-1-0016 (to R.K.J.)."

www.pnas.org/cgi/doi/10.1073/pnas.1400494111

Generation of functionally competent and durable engineered blood vessels from human induced pluripotent stem cells

Rekha Samuel[a,1,2], Laurence Daheron[b,2], Shan Liao[a,2], Trupti Vardam[a,2], Walid S. Kamoun[a], Ana Batista[a], Christa Buecker[b,3], Richard Schäfer[b,3], Xiaoxing Han[a], Patrick Au[a,4], David T. Scadden[c], Dan G. Duda[a], Dai Fukumura[a,5], and Rakesh K. Jain[a,5]

[a]Edwin L. Steele Laboratory, Department of Radiation Oncology, Massachusetts General Hospital, Boston, MA 02114; [b]Department of Stem Cell and Regenerative Biology, Harvard Stem Cell Institute, Harvard University, Cambridge, MA 02138; and [c]Center for Regenerative Medicine, Richard B. Simches Research Center, Massachusetts General Hospital, Boston, MA 02114

Contributed by Rakesh K. Jain, June 6, 2013 (sent for review February 1, 2013)

Efficient generation of competent vasculogenic cells is a critical challenge of human induced pluripotent stem (hiPS) cell-based regenerative medicine. Biologically relevant systems to assess functionality of the engineered vessels in vivo are equally important for such development. Here, we report a unique approach for the derivation of endothelial precursor cells from hiPS cells using a triple combination of selection markers—CD34, neuropilin 1, and human kinase insert domain-containing receptor—and an efficient 2D culture system for hiPS cell-derived endothelial precursor cell expansion. With these methods, we successfully generated endothelial cells (ECs) from hiPS cells obtained from healthy donors and formed stable functional blood vessels in vivo, lasting for 280 d in mice. In addition, we developed an approach to generate mesenchymal precursor cells (MPCs) from hiPS cells in parallel. Moreover, we successfully generated functional blood vessels in vivo using these ECs and MPCs derived from the same hiPS cell line. These data provide proof of the principle that autologous hiPS cell-derived vascular precursors can be used for in vivo applications, once safety and immunological issues of hiPS-based cellular therapy have been resolved. Additionally, the durability of hiPS-derived blood vessels in vivo demonstrates a potential translation of this approach in long-term vascularization for tissue engineering and treatment of vascular diseases. Of note, we have also successfully generated ECs and MPCs from type 1 diabetic patient-derived hiPS cell lines and use them to generate blood vessels in vivo, which is an important milestone toward clinical translation of this approach.

diabetes | vascular endothelial cells | reprogramming

Vascular disease is the principal cause of mortality in the United States. More than one in three Americans (36.9%) suffer from heart disease, and by 2030, an estimated 116 million people in the United States (40.5%) will have some form of cardiovascular disease. By this time, the cost of medical care for heart disease is expected to increase from $273 billion to $818 billion (1). Cell-based vascular regenerative engineering is an attractive option for revascularization that requires further validation before clinical translation (2). The discovery of human induced pluripotent stem (hiPS) cells (3, 4) has brought great hope because of their capacity to differentiate into different cell types and great potential for use in tissue engineering and regeneration (5). Several protocols to derive endothelial and perivascular lineages have been reported, with varying efficiencies (6–11). Disease-specific hiPS cells may serve as an excellent source for modeling human diseases (4, 12, 13). Indeed, the hiPS cell-derived vascular precursor cells have been shown to be excellent models to study disease. For example, hiPS cell-derived vascular precursors have been used to derive blood–brain barrier type endothelial cells (ECs) in culture (14) or to study patient-specific EC and smooth muscle cell defects in a Hutchinson Gilford progeria model (15) and rescue the vascular phenotype of Williams–Beuren syndrome (16).

Moreover, hiPS cell-derived endothelial precursor cells (EPCs) have been shown to alleviate myocardial insufficiency in bovine models (10) and peripheral arterial disease in murine models (9) and to improve recovery of blood flow in hind-limb ischemia murine models (11). Additionally, a recent hiPS derivation of EPCs using partially reprogrammed fibroblasts, demonstrated a quick reprogramming to ECs and the potential application for acute critical limb ischemia (11). There are applications in cell therapy-based regenerative medicine, where sustained, durable, and functionally competent blood vessels are crucial, such as in long-standing ischemic (17), arterial, diabetic, or nonhealing ulcers. Lack of timely intervention thereof leads to nontraumatic limb amputation (18).

A prerequisite to realize the full potential of hiPS cell-derived EPCs in forming blood vessels is the ability to examine their functional characteristics in vivo. To this end, we first optimized selection markers and a culture system for efficient expansion of hiPS cell-derived EPCs. Then, we tested the vasculogenic capacity of hiPS cell-derived EPCs in a model of durable blood vessel formation in vivo in mice using a murine embryonic precursor cell line, 10T1/2, as supporting perivascular cells (19). Next, we determined whether mesenchymal precursor cells (MPCs) could be derived from hiPS cells and if they could support vasculogenesis when coimplanted with hiPS ECs in vivo. Finally, we tested whether hiPS cells derived from patients harboring diseases with potential vascular complications, such as type 1 diabetes (T1D),

Author contributions: R. Samuel, D.G.D., D.F., and R.K.J. designed research; R. Samuel, S.L., T.V., W.S.K., A.B., C.B., R. Schäfer, and X.H. performed research; R. Samuel, L.D., S.L., T.V., W.S.K., A.B., P.A., D.T.S., D.G.D., D.F., and R.K.J. analyzed data; and R. Samuel, D.G.D., D.F., and R.K.J. wrote the paper.

Conflict of interest statement: R.K.J. received research grants from Dyax, MedImmune, and Roche; received consultant fees from Enlight, Noxxon, SynDevRx, WebMD, and Zyngenia; owns equity in Enlight, SynDevRx, and XTuit; and serves on the Board of Directors of XTuit and the Board of Trustees of H&Q Healthcare Investors and H&Q Life Sciences Investors. No reagents or funding from these companies was used in these studies; therefore, there is no significant financial or other competing interest in the work.

Freely available online through the PNAS open access option.

[1]Present address: Centre for Stem Cell Research, Christian Medical College, Bagayam, Vellore 632002, Tamil Nadu, India.

[2]R. Samuel, L.D., S.L., and T.V. contributed equally to this work.

[3]Present address: Department of Neurosurgery, Stanford University School of Medicine, Stanford, CA 94305.

[4]Present address: Office of Cellular, Tissue, and Gene Therapies, US Food and Drug Administration, Rockville, MD 20852.

[5]To whom correspondence may be addressed. E-mail: dai@steele.mgh.harvard.edu or jain@steele.mgh.harvard.edu.

This article contains supporting information online at www.pnas.org/lookup/suppl/doi:10.1073/pnas.1310675110/-/DCSupplemental.

can be differentiated to ECs and MPCs and if these progenies have vasculogenic potential.

Results

Differentiated hiPS Cells Coexpressing CD34, human kinase insert domain-containing receptor, and Neuropilin 1 Are Enriched in EPCs. We first established a robust protocol for EPC derivation. The previously established method for EC differentiation from hESCs using CD34 sorting (20) was not optimal for hiPS cells (*SI Appendix*, Table S1). Thus, we sorted the $CD34^+$ cell subpopulation coexpressing the early EPC markers neuropilin 1 (NRP1) (21) and VEGF receptor 2, human kinase insert domain-containing receptor (KDR) (22). We separated five subpopulations of cells ($CD34^+KDR^+NRP1^+$, $CD34^-KDR^-NRP1^-$, $CD34^+KDR^-NRP1^-$, $CD34^-KDR^-NRP1^+$, and $CD34^-KDR^+NRP1^+$ cells) by flow cytometry (*SI Appendix*, Figs. S1 and S2) and derived them from four hiPS cell lines: human adult dermal fibroblast cell line (HFib2)-iPS4, HFib2-iPS5, human foreskin fibroblast cell line (HS27)-iPS, and human foreskin fibroblast cell line (BJ)-iPS cells (*SI Appendix*, *SI Materials and Methods*, section I.A). We found the peak in the number of $CD34^+KDR^+NRP1^+$ differentiated HS27-iPS cells (i.e., 3.3%) at day 7. We first tested the capacity of these cell populations to differentiate into ECs using a 2D culture system (Fig. 1 *A*–*C*). Only the cells derived from $CD34^+KDR^+NRP1^+$ cells showed bona fide characteristics of ECs. These cells expressed the endothelial markers CD31, CD144, and von Willebrand factor, and they showed uptake of acetylated (Ac)-LDL and tube formation on Matrigel (Fig. 1 *D*–*H*). The HS27-iPS cell derivatives with the other four populations lacked these endothelial characteristics and displayed a fibroblast-like morphology and increased senescence (*SI Appendix*, *SI Materials and Methods* and Fig. S3). The $CD34^+KDR^+NRP1^+$ cell-derived ECs could be expanded for up to 15 passages while maintaining angiogenic gene expression (*SI Appendix*, *SI Materials and Methods* and Fig. S4*A*) and characteristic "cobblestone" endothelial morphology in monolayers. Similar results were obtained with three other healthy donor-derived hiPS cell lines (BJ-iPS, HFib2-iPS4, and HFib2-iPS5). However, the HS27-iPS cell line showed a higher propensity for EC derivation and in vivo functionality compared with the other hiPS cell lines (*SI Appendix*, Fig. S5), and it was used for the subsequent in vivo studies.

hiPS Cell-Derived ECs Can Form Functional Blood Vessels in Vivo. Next, using a previously established tissue-engineered blood vessel model (19), we evaluated the vasculogenic potential and monitored in real time the structure and function of vessels formed by hiPS cell-derived ECs by means of intravital multiphoton microscopy in SCID mice. The $CD34^+KDR^+NRP1^+$ cell-derived ECs were expanded in vitro for up to 10 d before implantation in vivo in the cranial window model to generate adequate cell numbers for implantation (*SI Appendix*, *SI Materials and Methods*). Although hiPS cells were initially sorted based on their expression of CD34, KDR, and NRP1, the progenies of this population after in vitro culture for 10 d showed a low level of CD34 expression (*SI Appendix*, Fig. S4*B*). These data indicate that the $CD34^+KDR^+NRP1^+$ cell population is enriched in EPCs, which acquired a more mature EC phenotype during the 10-d culture period.

hiPS cell-derived ECs coimplanted with 10T1/2 MPCs formed blood-perfused vessels within 2 wk postimplantation in vivo (Fig. 2*A*, *SI Appendix*, and Movies S1 and S2). Once vascular network formation was completed, vessels became mature and stable, and densities of ECs and supporting cells remained relatively constant (*SI Appendix*, Fig. S6). Whole-mount gel staining at 6 mo postimplantation showed an infiltration of the gel by the host $CD31^+$ murine ECs, which anastomosed with the engineered vessels at the host–implant interface (Fig. 3*A*), as recently described, via stabilization or a "wrapping and tapping" mechanism (23). The engineered vessels were associated with both implanted 10T1/2 supporting cells and desmin-positive host-derived cells (Fig. 3*B*). Of note, ECs derived from hiPS cells showed no vasculogenic potential when implanted alone (i.e., without MPC support). Functional intravital microscopy analyses showed that the engineered vessels demonstrated RBC velocity and flux comparable to capillaries and exchange vessels in the adjacent brain tissues (Fig. 2 *B* and *C*). Further studies showed that 4 wk after gel implantation in cranial windows, 68% of the mice ($n = 25$) implanted with hiPS-ECs and 10T1/2 cells formed functional vessels. The RBC velocities were measured in 5 of those mice (1.36 ± 0.3 mm/s), and they were comparable to those of normal capillaries or postcapillary venules (24). The engineered vessels from $CD34^+KDR^+NRP1^+$ hiPS

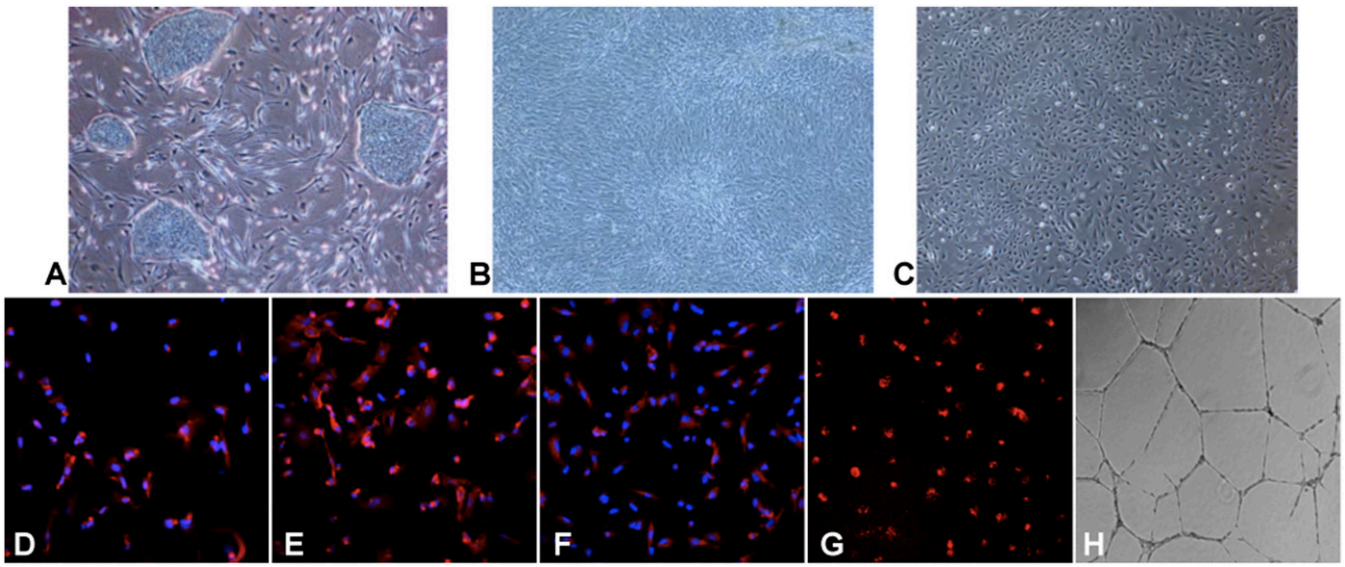

Fig. 1. Differentiation and characterization of hiPS cell-derived ECs. (*A*–*C*) 2D EC differentiation from nondiseased hiPS cells. (*A*) HS27-iPS cell colonies grown on feeder cells (mouse embryonic fibroblasts). (*B*) Day 10 in differentiation medium (50 ng/mL bone morphogenetic protein-4 added on day 1). (*C*) Putative EC morphology. Immunocytochemical staining of HS27-iPS-ECs for CD31 (*D*), vascular endothelial cadherin (*E*), and von Willebrand factor (*F*). (*G*) HS27-iPS-ECs show uptake for Ac-LDL. (*H*) HS27-iPS-ECs show tube formation on Matrigel. (Magnification: *A*–*G*, 10×.)

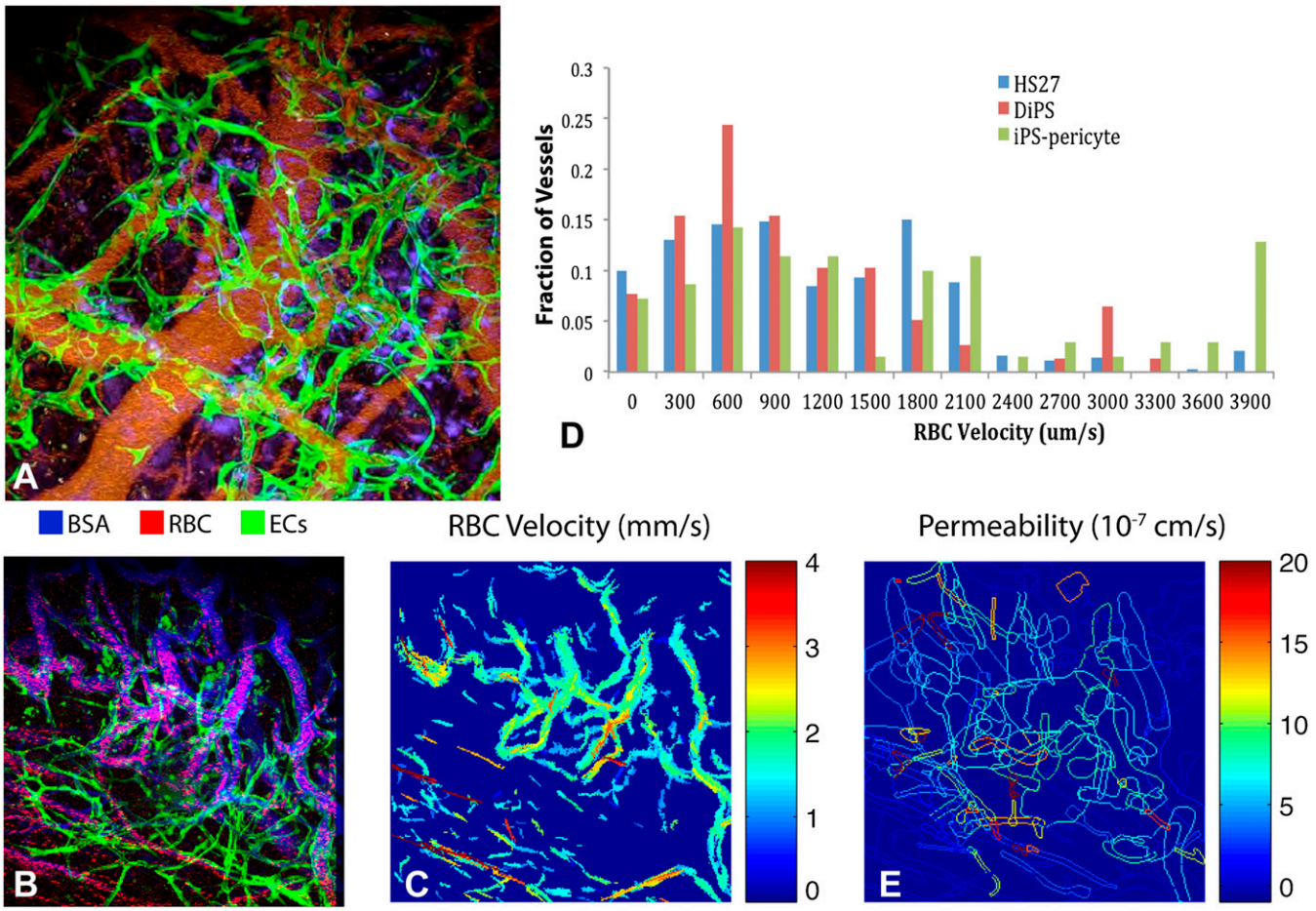

Fig. 2. In vivo imaging of hiPS cell-derived engineered blood vessels. (*A*) Multiphoton laser-scanning microscopy image of HS27-iPS-ECs (green) and 10T1/2 cells (blue) coembedded in a fibronectin/collagen I tissue-engineered vessel construct and inoculated in SCID mice in a cranial window. These cells developed functional perfused blood vessels [red, 1,1-dioctadecyl-3,3,3,3-tetramethylindodicarbocyanine perchlorate (DID)-labeled RBCs] in vivo (day 14). (*B–D*) Functional assessment of iPS cell-derived engineered blood vessels. (*B*) Perfused vessels engineered from HS27-iPS-ECs (green) imaged after injection of DiD-RBCs (red) and Alexa 647-BSA (blue). (*C*) Map of RBC velocity quantified by recently established line and full-field RBC velocity-scanning techniques (45). Engineered vessels are well perfused. (*D*) Histogram of RBC velocity profile in iPS cell-derived vessels. HS27-iPS-ECs with 10T1/2 cells (blue bars), T1D-iPS-ECs with 10T1/2 cells (brown bars), and HS27-iPS-ECs with HS27-iPS-mesenchymal cells (green bars) are shown. (*E*) Map of vessel permeability to Alexa 647-labeled BSA quantified based on the extravasation of BSA from individual vessels over time. Engineered vessels have a segment with higher permeability compared with endogenous normal vessels. Multiphoton imaging was carried out on a custom-built multiphoton laser-scanning microscope using a confocal laser-scanning microscope body and a broadband femtosecond laser source. Imaging studies in *A*–C and *E* were performed at a magnification of 20×, using a 0.95-N.A. water immersion objective. Two-micron-thick optical sections were taken. The imaging field of view was 660 μm × 660 μm × 155 μm with a resolution of 1.3 μm × 1.3 μm × 2 μm.

cell-derived ECs lasted in vivo for 280 d, in sharp contrast to the other hiPS cell derivatives, which regressed within a few days (Fig. 4*A*).

In addition, we performed s.c. implants of hiPS cell-derived ECs in Matrigel plugs. Whereas hiPS cell-derived ECs coimplanted with 10T1/2 cells formed RBC-perfused blood vessels (*SI Appendix*, Figs. S7 *A* and *B*), there was no appreciable vessel formation in Matrigel plugs implanted without any cells (*SI Appendix*, Fig. S7*C*) or with the hiPS cell-derived ECs alone. Histological examination of the s.c. gel in the dorsal chamber at day 30 showed perfused blood vessels containing RBCs in the lumen (*SI Appendix*, Fig. S8). However, vasculogenesis in this model required fivefold higher numbers of both hiPS cell-derived ECs and 10T1/2 cells in the construct. This result is consistent with our previous data showing that s.c. implantation requires higher doses of angiogenic factors for new vessel formation compared with the brain (25). Of note, we did not observe teratoma formation in any of the in vivo experiments.

Generation of ECs and Blood Vessels in Vivo from Patient-Derived hiPS Cells. Having established that hiPS-derived ECs from healthy individuals can form durable and functional vasculature in vivo, we next tested whether hiPS from patients with disease who potentially develop vascular complications can do the same. To this end, we separated $CD34^+KDR^+NRP1^+$ cells from four T1D-iPS cell lines derived from patients with T1D (1021-4F-B-DiPS, 1024-4F-2A-DiPS, 1027-3F-C-DiPS, and 1028-3F-A-DiPS) and expanded them using the 2D protocol (*SI Appendix*, *SI Materials and Methods*).

We next implanted the bona fide ECs derived from T1D-iPS cells (*SI Appendix*, Fig. S9) with 10T1/2 MPCs in vivo using the tissue-engineered model in the cranial window of SCID mice (26, 27). We found that T1D-iPS cell-derived ECs could generate a functional vasculature within 2 wk of coimplantation. Established T1D-iPS cell-derived blood vessels also persisted for the entire period of observation (120 d) in mice and demonstrated good perfusion of RBCs in the engineered vessels derived from T1D-iPS-ECs (Fig. 2*D*, *SI Appendix*, and Movies S3 and S4).

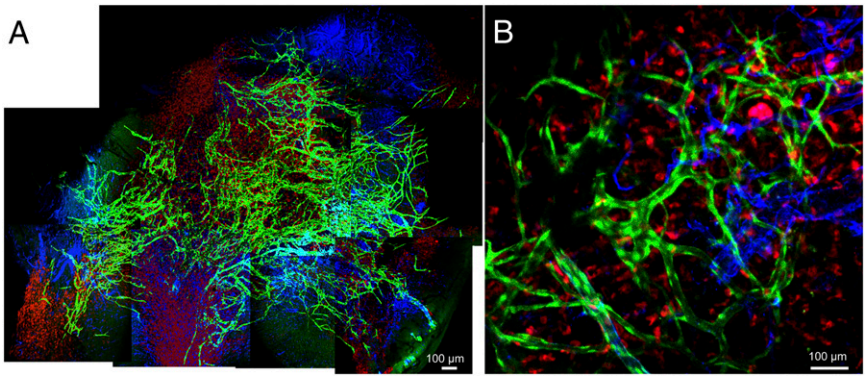

Fig. 3. Tissue imaging of engineered vessel construct. (*A*) Confocal whole-mount image of the tissue-engineered vessel construct (collagen 1 gel) extracted from the cranial window of an SCID mouse after 6 mo. Eleven images (all 20x) were manually aligned to form this mosaic image. EGFP$^+$ HS27-iPS-ECs (green) are forming vessels with DsRed$^+$ 10T1/2 supporting cells (red). Mouse CD31$^+$ host ECs (blue) infiltrated in the gel and anastomosed with engineered vasculature (green). (*B*) High-power confocal image of the excised engineered vessel construct with EGFP$^+$ HS27-iPS-ECs (green) and DsRed$^+$ 10T1/2 supporting cells (red). In this image, desmin-positive perivascular cells surrounding engineered vessels (blue) are shown.

Moreover, the T1D-iPS-EC vessels were not apparently leaky similar to those in the nondiseased hiPS-EC vessels or the engineered vessels derived from other sources of ECs (19).

Mesenchymal Cells Derived from hiPS Cells Can Support hiPS-EC–Engineered Vessels. Because mesenchymal cells are essential for functional and durable vessel formation, deriving them from clinically accessible precursors, such as hiPS cells, would be a critical step for the translation of this tissue-engineered vessel approach in patients (28). To test the possible use of mesenchymal cells derived from hiPS cells in the engineered vessel model, we isolated CD73$^+$ cells from the CD31$^-$CD144$^-$ fraction of differentiated HS27-iPS cells and expanded them in human mesenchymal stem cell (MSC) medium for a period of 2 wk (*SI Appendix*, *SI Materials and Methods*). Flow cytometric analysis confirmed that these cells had the phenotype of MPCs, as demonstrated by expression of CD90, CD105, and CD44 and lack of expression of CD144, CD31, and CD45 (*SI Appendix*, Fig. S10). Moreover, these hiPS cell-derived MPCs displayed adipocytic, chondrocytic, and osteoblastic differentiation when exposed to the appropriate media in vitro (*SI Appendix*, Fig. S11), similar to bone marrow-derived human MSCs obtained from Cambrex Bioscience (catalog no. PT-3238). We next coimplanted the HS27-iPS cell-derived MPCs with the same hiPS cell-derived ECs to test their vasculogenic potential in vivo. Indeed, the hiPS cell-derived MPCs could support the formation of durable and functional vessels (*SI Appendix*, Fig. S12 and Movie S5) for more than half of the mice over 28 d (*SI Appendix*, Fig. S13), which is 2.5-fold longer than human MSCs derived from bone marrow (catalog. no. PT-3238) (Fig. 4*B*). We were unable to derive MPCs from T1D-iPS cells using our original 2D protocol. However, we could derive MPCs from one of the four T1D-iPS cell lines (1024-4F-2A-DiPS), using an alternate 2D protocol and sorting CD73$^+$ cells (*SI Appendix*, *SI Materials and Methods*, section I.D). This result highlights the importance of individual cell line variability, as well as differentiation protocols that affect the differentiation potential of hiPS cell vascular derivatives. The 1024-4F-2A-DiPS-MPCs formed functional blood vessels when coimplanted with human umbilical cord vein endothelial cells (HUVECs) by day 16 (*SI Appendix*, Figs. S14 and S16). These MPCs were indeed capable of supporting engineered blood vessels in vivo similar to 10T1/2 cells, which are the current gold standard (*SI Appendix*, Fig. S17). These findings support the potential of using human sources of ECs and MPCs in regenerative medicine for patients with vascular diseases.

Discussion

Cell-based vascular engineering for tissue repair/regeneration involves the incorporation of vascular precursor cells within biomaterials to restore integrity of blood vessels or generate new blood vessels (2). We previously reported successful generation of durable engineered blood vessels in vivo using HUVECs (19) or ECs derived from cord blood-derived EPCs (26) or hESCs (20). In all cases, coimplantation with murine MPC 10T1/2 cells (19, 20, 26) or human MSCs (29) was required to sustain these engineered blood vessels in vivo.

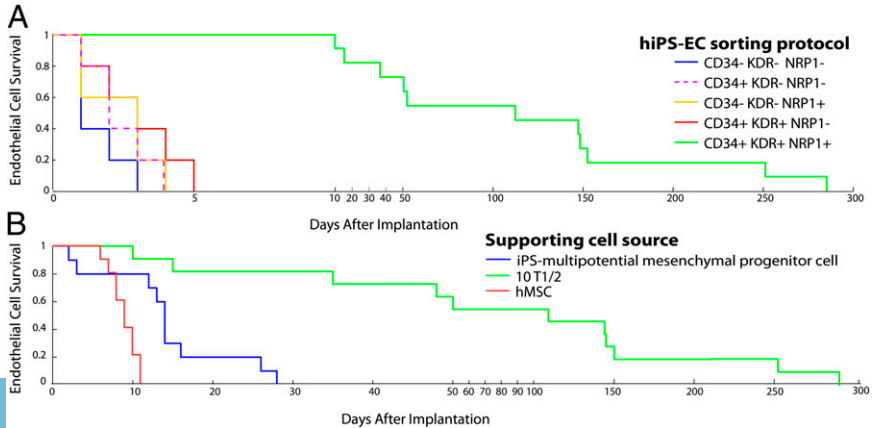

Fig. 4. In vivo lifetime of engineered vessels. (*A*) In vivo Kaplan–Meier survival curves of ECs derived from HS27-iPS cell 2D differentiation with different sorting protocols. The fraction of mice containing viable ECs in each group at a given time point is presented. Maximum in vivo EC survival was seen with the CD34$^+$KDR$^+$NRP1$^+$ protocol group (up to 280 d). (*B*) In vivo Kaplan–Meier survival curves of engineered vessels derived from HS27-iPS-ECs coimplanted with mesenchymal progenitor cells for different sources. HS27-iPS cell-derived multipotent mesenchymal progenitor cells showed longer duration of durable blood vessels (~28 d) compared with bone marrow-derived human MSCs (hMSCs), which could support engineered vessels for only ~11 d.

Translation of our previous findings will thus require patient-compatible sources of both ECs and mesenchymal cells in a large quantity. Unfortunately, the likelihood of having a patient's own HUVECs or cord blood EPCs accessible for use in regenerative medicine in adulthood is currently remote. Moreover, the ethical concerns surrounding the use of hESC-derived ECs currently preclude their application in many countries. Yamanaka's breakthrough discovery of hiPS cells in 2007 (4) provided a potential inexhaustible source of vascular cells that could avert the immunological and ethical controversies that surround the use of human ECs derived from other sources. Recent development of viral-free and nonintegrating approaches for generation of safe hiPS cells makes this a real possibility (30).

Surprisingly, the functional capacity of hiPS-derived ECs in vivo in a noninvasive model has not yet been explored (6, 7). In addition, the vasculogenic potential of different stem cell lines appears to be much more variable for hiPS cells than for hESCs, and this could have a direct impact on differentiation capability (31). We have previously reported on a recently developed 2D approach of deriving ECs from hESCs using CD34 sorting, implicating CD34 as a primitive EPC marker (20). $CD34^+$ progenitor cells from peripheral blood appear to be a popular starting material from which to derive hiPS cells (32). We used magnetic bead sorting to obtain up to 6% $CD34^+$ cells using the healthy hiPS cell lines (*SI Appendix*, Table S1), and we used endothelial differentiation culture conditions as described for hESCs (20). In our experience, the hiPS-ECs derived from $CD34^+$ cells were unable to expand further in culture. In this study, we show that presorting of hiPS cell-derived EPCs using a combination of three markers—CD34, KDR, and NRP1—allowed generation of large numbers of bona fide ECs endowed with in vivo potential of functional vessel formation. NRP1 has been shown to be expressed in EPCs and before CD34 in hESCs (21), and isolated embryonic KDR^+ cells are believed to be primitive EPCs (22). Recently, KDR^+ cells have been shown to yield a pure EC population from hESCs and hiPS cells (33). We therefore explored whether a combination of these markers—CD34, NRP1, and KDR—had primitive vasculogenic potential in vivo using a 2D approach for generating ECs. Indeed, the $CD34^+$ KDR^+NRP1^+ ECs formed durable blood vessels (over 280 d) in mice, indicating an exciting potential of this approach for vascular tissue engineering.

Although various 3D culture systems (e.g., embryoid bodies) have been proposed for efficient generation of ECs (8), we found that a 2D approach is far more efficient than a 3D method for EC derivation from hESCs (20). However, the superiority of 2D culture was not known for iPS-EC differentiation. To this end, we compared our 2D method with an established two-step 3D and 2D protocol for EC differentiation (*SI Appendix*, *SI Materials and Methods*). The dual 3D and 2D in vitro method successfully differentiated hiPS cels into EPCs, and ultimately into ECs (*SI Appendix*, Figs. S18 and S19). However, ECs derived from the 3D method failed to form stable blood vessels in vivo (*SI Appendix*, Fig. S20). This confirms that the 2D culture method is more efficient in deriving vasculogenic ECs from hiPS cells and emphasizes the importance of in vivo testing of hiPS cell progenies.

Using autologous ECs derived from patients with vascular complications would be challenging (34). Hence, we next explored generation of ECs in hiPS cells derived from individuals with disease and their capacity to form functional blood vessels in vivo. It is known that T1D is associated with dysfunctional ECs (34). Although the current focus of iPS technology for T1D is on the generation of functional pancreatic islet cells for cell replacement therapy (35), interestingly, circulating EC function was found to improve after the islet cell transplantation (36). In line with those findings, we successfully generated functional blood vessels in vivo using ECs derived from three different T1D-iPS cell lines. Such capability to generate large amounts of functional EPCs from patients for autologous cell transplantation or tissue-engineering strategies is highly appealing not only for T1D but for many diseases where revascularization is required.

Functional stable vasculature for tissue engineering requires both ECs and a perivascular source, vascular smooth muscle, MSC, pericyte, or MPC (37). It is therefore equally relevant to obtain perivascular cells from hiPS cells (38). In this study, we could generate MPCs, which can function as perivascular supporting cells in vivo, from healthy or T1D-iPS cells. This development further supports the potential use of hiPS-derived MPCs in regenerative medicine. However, these MPCs are not as robust as 10T1/2 cells, the most potent MPCs we have tested to date. Hence, further studies to identify the mechanisms that define the in vivo efficiency of MPCs are warranted.

Having highlighted the clinical potential of these hiPS-derived ECs and MPCs, as well as their vasculogenic capacity, a number of concerns must be addressed before their clinical translation. For example, the ability to generate durable blood vessels from different iPS cells is quite variable despite the uniform ability to generate bona fide ECs in vitro using the same method of triple selection for $CD34^+$, KDR^+, and $NRP1^+$ with the 2D differentiation protocol. Our gene expression profile analyses did not detect significant differences between vasculogenic and non-vasculogenic hiPS-ECs (*SI Appendix*, Table S2). Further dissection of molecular determinants of in vivo fate (the ability to form and maintain engineered vessels) of these seemingly bona fide ECs is warranted. Another consideration is that current in vivo methods to test for blood vessel formation and vascular function are performed not in a diseased host but in healthy immunodeficient animals. Host immune environment affects the functionality of engineered vessels (39). Furthermore, the host environment in patients with disease, such as those with diabetes, is not as supportive for vasculogenesis as in a healthy host (40). For further development of the hiPS-EC–based strategy, the use of syngeneic disease-specific models might be necessary (41).

In summary, we have generated hiPS cell-derived ECs capable of forming blood vessels in vivo from various hiPS cell lines. We have successfully engineered functional blood vessels from ECs and MPCs derived from the same healthy hiPS cell line. Additionally, we showed that hiPS cell-derived ECs and perivascular MPCs from patients with T1D may have differential vasculogenic potential in vivo. Taken together, these findings suggest that autologous hiPS cell-derived vascular precursors could potentially be used to treat vascular disease in cell-based vascular regenerative engineering.

Materials and Methods

HiPS cell lines were generated by transducing various combinations of octamer-binding transcription factor-4 (Oct-4), sex determining region Y, box 2 (Sox-2, also known as SRY), kruppel-like factor 4 (Kfl-4), cellular homolog of the myelocytomatosis viral oncogene (c-myc), and Nanog to fibroblasts (3, 42, 43). ECs were differentiated from these hiPS cells by 2D (20) or 3D (44) culture methods and sorted by flow cytometry using combinations of anti-CD34, KDR, and NRP1 antibodies. For MPCs, $CD73^+CD31^-CD144^-$ or $CD73^+$ cells were isolated after 2D differentiation of hiPS cells. Molecular and immunocytochemical analyses, cell senescence, Ac-LDL uptake, and in vitro tube formation assays were performed as described in *SI Appendix*, *SI Materials and Methods*. In vivo vasculogenic potential of hiPS cell-derived ECs and MPCs was determined using a tissue-engineered vessel model, intravital microscopy, and immunohistochemistry, as described in *SI Appendix*, *SI Materials and Methods*. All animal procedures were carried out following the Public Health Service Policy on Humane Care of Laboratory Animals and approved by the Institutional Animal Care and Use Committee of Massachusetts General Hospital.

In *SI Appendix* and Movies S1, S2, S3, S4, S5, and S6, multiphoton imaging was carried out on a custom-built multiphoton laser-scanning microscope using a confocal laser-scanning microscope body (Olympus 300; Optical Analysis) and a broadband femtosecond laser source (High Performance MaiTai; Spectra-Physics). Imaging studies were performed with a magnification of 20× and a 0.95-N.A. water immersion objective (Olympus XLUMPlanFI, 1-UB965; Optical Analysis). Multiple regions of interest were randomly

chosen, ensuring that areas within the gel, at the periphery of the gel, and outside the gel were included. Two-micron-thick optical sections were taken. The imaging field of view was 660 μm × 660 μm × 155 μm with a resolution of 1.3 μm × 1.3 μm × 2 μm.

ACKNOWLEDGMENTS. We thank Sylvie Roberge, Peigen Huang, Christina Koppel, Phyllis McNally, and Julia Kahn for outstanding technical assistance and Drs. Vikash Pal Singh Chauhan, Ravi Mylvaganam, and Matija Snuderl for help with the experiments. We also thank Dr. Douglas Melton for his generous gift of T1D-iPS cell lines and helpful scientific input on our manuscript. This work was supported by a fellowship from the Department of Biotechnology, Ministry of Science and Technology, Government of India (to R. Samuel); a Tosteson Postdoctoral Fellowship, Charles A. King Trust Fellowship, and Grant K99HL111343-01A1 (to S.L.); funds from the Harvard Stem Cell Institute; National Institutes of Health Grant P01-CA080124; Federal Share/National Cancer Institute Proton Beam Program Income Grants R01-CA115767, R01-CA085140, and R01-CA126642 (to R.K.J.), R01CA159258 (to D.G.D.), and R01-CA096915 (to D.F.); and American Cancer Society Grant 120733-RSG-11-073-01-TBG (to D.G.D.).

1. Heidenreich PA, et al.; American Heart Association Advocacy Coordinating Committee; Stroke Council; Council on Cardiovascular Radiology and Intervention; Council on Clinical Cardiology; Council on Epidemiology and Prevention; Council on Arteriosclerosis; Thrombosis and Vascular Biology; Council on Cardiopulmonary; Critical Care; Perioperative and Resuscitation; Council on Cardiovascular Nursing; Council on the Kidney in Cardiovascular Disease; Council on Cardiovascular Surgery and Anesthesia, and Interdisciplinary Council on Quality of Care and Outcomes Research (2011) Forecasting the future of cardiovascular disease in the United States: A policy statement from the American Heart Association. *Circulation* 123(8):933–944.
2. Kusuma S, Gerecht S (2010) Engineering blood vessels using stem cells: Innovative approaches to treat vascular disorders. *Expert Rev Cardiovasc Ther* 8(10):1433–1445.
3. Takahashi K, et al. (2007) Induction of pluripotent stem cells from adult human fibroblasts by defined factors. *Cell* 131(5):861–872.
4. Yamanaka S (2007) Strategies and new developments in the generation of patient-specific pluripotent stem cells. *Cell Stem Cell* 1(1):39–49.
5. Cherry AB, Daley GQ (2013) Reprogrammed cells for disease modeling and regenerative medicine. *Annu Rev Med* 64:277–290.
6. Feng Q, et al. (2010) Hemangioblastic derivatives from human induced pluripotent stem cells exhibit limited expansion and early senescence. *Stem Cells* 28(4):704–712.
7. Drukker M, et al. (2012) Isolation of primitive endoderm, mesoderm, vascular endothelial and trophoblast progenitors from human pluripotent stem cells. *Nat Biotechnol* 30(6):531–542.
8. James D, et al. (2010) Expansion and maintenance of human embryonic stem cell-derived endothelial cells by TGFbeta inhibition is Id1 dependent. *Nat Biotechnol* 28(2):161–166.
9. Rufaihah AJ, et al. (2011) Endothelial cells derived from human iPSCS increase capillary density and improve perfusion in a mouse model of peripheral arterial disease. *Arterioscler Thromb Vasc Biol* 31(11):e72–e79.
10. Templin C, et al. (2012) Transplantation and tracking of human-induced pluripotent stem cells in a pig model of myocardial infarction: Assessment of cell survival, engraftment, and distribution by hybrid single photon emission computed tomography/computed tomography of sodium iodide symporter transgene expression. *Circulation* 126(4):430–439.
11. Margariti A, et al. (2012) Direct reprogramming of fibroblasts into endothelial cells capable of angiogenesis and reendothelialization in tissue-engineered vessels. *Proc Natl Acad Sci USA* 109(34):13793–13798.
12. Park IH, et al. (2008) Disease-specific induced pluripotent stem cells. *Cell* 134(5):877–886.
13. Unternaehrer JJ, Daley GQ (2011) Induced pluripotent stem cells for modelling human diseases. *Philos Trans R Soc Lond B Biol Sci* 366(1575):2274–2285.
14. Lippmann ES, et al. (2012) Derivation of blood-brain barrier endothelial cells from human pluripotent stem cells. *Nat Biotechnol* 30(8):783–791.
15. Zhang J, et al. (2011) A human iPSC model of Hutchinson Gilford Progeria reveals vascular smooth muscle and mesenchymal stem cell defects. *Cell Stem Cell* 8(1):31–45.
16. Kinnear C, et al. (2013) Modeling and rescue of the vascular phenotype of Williams-Beuren syndrome in patient induced pluripotent stem cells. *Stem Cells Transl Med* 2(1):2–15.
17. Ohno T, Kaneda H, Nagai Y, Fukushima M (2012) Regenerative medicine in critical limb ischemia. *J Atheroscler Thromb* 19(10):883–889.
18. Morbach S, et al. (2012) Long-term prognosis of diabetic foot patients and their limbs: Amputation and death over the course of a decade. *Diabetes Care* 35(10):2021–2027.
19. Koike N, et al. (2004) Tissue engineering: Creation of long-lasting blood vessels. *Nature* 428(6979):138–139.
20. Wang ZZ, et al. (2007) Endothelial cells derived from human embryonic stem cells form durable blood vessels in vivo. *Nat Biotechnol* 25(3):317–318.
21. Cimato T, et al. (2009) Neuropilin-1 identifies endothelial precursors in human and murine embryonic stem cells before CD34 expression. *Circulation* 119(16):2170–2178.
22. Sun X, Cheng L, Duan H, Lin G, Lu G (2012) Characterization and comparison of embryonic stem cell-derived KDR+ cells with endothelial cells. *Microvasc Res* 84(2):149–154.
23. Cheng G, et al. (2011) Engineered blood vessel networks connect to host vasculature via wrapping-and-tapping anastomosis. *Blood* 118(17):4740–4749.
24. Yuan F, et al. (1994) Vascular permeability and microcirculation of gliomas and mammary carcinomas transplanted in rat and mouse cranial windows. *Cancer Res* 54(17):4564–4568.
25. Dellian M, Witwer BP, Salehi HA, Yuan F, Jain RK (1996) Quantitation and physiological characterization of angiogenic vessels in mice: Effect of basic fibroblast growth factor, vascular endothelial growth factor/vascular permeability factor, and host microenvironment. *Am J Pathol* 149(1):59–71.
26. Au P, et al. (2008) Differential in vivo potential of endothelial progenitor cells from human umbilical cord blood and adult peripheral blood to form functional long-lasting vessels. *Blood* 111(3):1302–1305.
27. Au P, Tam J, Fukumura D, Jain RK (2007) Small blood vessel engineering. *Methods Mol Med* 140:183–195.
28. Eberle I, Moslem M, Henschler R, Cantz T (2012) Engineered MSCs from patient-specific iPS cells. *Adv Biochem Eng Biotechnol*, 10.1007/10_2012_156.
29. Au P, Tam J, Fukumura D, Jain RK (2008) Bone marrow-derived mesenchymal stem cells facilitate engineering of long-lasting functional vasculature. *Blood* 111(9):4551–4558.
30. Warren L, et al. (2010) Highly efficient reprogramming to pluripotency and directed differentiation of human cells with synthetic modified mRNA. *Cell Stem Cell* 7(5):618–630.
31. Osafune K, et al. (2008) Marked differences in differentiation propensity among human embryonic stem cell lines. *Nat Biotechnol* 26(3):313–315.
32. Merling RK, et al. (2013) Transgene-free iPSCs generated from small volume peripheral blood nonmobilized CD34+ cells. *Blood* 121(14):e98–e107.
33. White MP, et al. (2013) Limited gene expression variation in human embryonic stem cell and induced pluripotent stem cell-derived endothelial cells. *Stem Cells* 31(1):92–103.
34. Loomans CJ, et al. (2004) Endothelial progenitor cell dysfunction: A novel concept in the pathogenesis of vascular complications of type 1 diabetes. *Diabetes* 53(1):195–199.
35. Alipio Z, et al. (2010) Reversal of hyperglycemia in diabetic mouse models using induced-pluripotent stem (iPS)-derived pancreatic beta-like cells. *Proc Natl Acad Sci USA* 107(30):13426–13431.
36. Petrelli A, et al. (2010) Improved function of circulating angiogenic cells is evident in type 1 diabetic islet-transplanted patients. *Am J Transplant* 10(12):2690–2700.
37. Carmeliet P, Jain RK (2011) Molecular mechanisms and clinical applications of angiogenesis. *Nature* 473(7347):298–307.
38. Bajpai VK, Mistriotis P, Loh YH, Daley GQ, Andreadis ST (2012) Functional vascular smooth muscle cells derived from human induced pluripotent stem cells via mesenchymal stem cell intermediates. *Cardiovasc Res* 96(3):391–400.
39. Chen RR, et al. (2007) Host immune competence and local ischemia affects the functionality of engineered vasculature. *Microcirculation* 14(2):77–88.
40. Waltenberger J (2001) Impaired collateral vessel development in diabetes: Potential cellular mechanisms and therapeutic implications. *Cardiovasc Res* 49(3):554–560.
41. Cao L, et al. (2010) Modulating Notch signaling to enhance neovascularization and reperfusion in diabetic mice. *Biomaterials* 31(34):9048–9056.
42. Park IH, Lerou PH, Zhao R, Huo H, Daley GQ (2008) Generation of human-induced pluripotent stem cells. *Nat Protoc* 3(7):1180–1186.
43. Buecker C, et al. (2010) A murine ESC-like state facilitates transgenesis and homologous recombination in human pluripotent stem cells. *Cell Stem Cell* 6(6):535–546.
44. Li Z, et al. (2009) Functional and transcriptional characterization of human embryonic stem cell-derived endothelial cells for treatment of myocardial infarction. *PLoS ONE* 4(12):e8443.
45. Kamoun WS, et al. (2010) Simultaneous measurement of RBC velocity, flux, hematocrit and shear rate in vascular networks. *Nat Methods* 7(8):655–660.